

Excitation Functions for the Fission Isomers ^{240m}Pu and ^{239m}Pu from $^{238}\text{U}(^4\text{He}, xn)$ Reactions*

M. N. Namboodiri,† F. H. Ruddy,‡ and John M. Alexander

Department of Chemistry, State University of New York at Stony Brook, Stony Brook, New York 11790

(Received 13 October 1972)

Excitation functions have been measured for the fission isomers ^{240m}Pu and ^{239m}Pu produced in the reactions of ^{238}U with ^4He . A value of 2.4 ± 0.5 nsec was obtained for the half-life of ^{240m}Pu . The high detection efficiency of thick targets and annular detector geometry has been used and refined. Upper limits of 0.3 and 0.6 μb have been obtained for the production of 29-nsec ^{240m}Pu and 6.5-nsec ^{239m}Pu , respectively.

I. INTRODUCTION

Spontaneously fissioning isomers have been the subject of several studies during the last ten years, and about 30 fission isomers have been characterized among the heavy elements.¹⁻⁶ It is believed that these isomers represent metastable states of the nucleus in a highly deformed shape.⁷⁻⁹ Measurements of half-lives and cross sections of isomers have been used to deduce parameters that describe the potential barrier to fission.^{5, 10-12} In particular, excitation functions have been used to deduce the excitation energy of the fission isomers.^{5, 9-12} This quantity is related to the energy difference between two minima in the fission barrier. Other parameters of the fission barrier have been estimated also. The analysis of excitation functions to obtain these parameters is carried out by comparison of experimental excitation functions to the results of a calculation based on a nuclear model. Detailed measurements of isomer excitation functions are important in this connection. The present paper reports the measurement of the excitation functions for ^{239m}Pu and ^{240m}Pu in the reaction $^{238}\text{U} + ^4\text{He}$. Dielectric track detectors and recoil techniques have been employed. A companion paper deals with the excitation functions for ^{239m}Am and ^{238m}Am in reactions ^{237}Np with ^4He .¹³ Statistical model calculations of these excitation functions, and the corresponding excitation functions for products in ground states, form the subject of a parallel investigation.¹⁴

The reactions $^{238}\text{U}(^4\text{He}, 2n)^{240m}\text{Pu}$ and $^{238}\text{U}(^4\text{He}, 3n)^{239m}\text{Pu}$ have been studied previously by Vandenbosch and Wolf³ and by Britt *et al.*⁵ The study by Vandenbosch and Wolf³ was aimed at the discovery and characterization of the isomers; they measured the cross sections only at a few selected energies. The more detailed measurements by Britt *et al.*⁵ were reported after the present work had been initiated. Britt *et al.* measured the ex-

citation function for ^{240m}Pu rather completely, but their measurements of ^{239m}Pu were confined to the low-energy side of the excitation function.

The results of Vandenbosch and Wolf³ suggested that the ^{239m}Pu excitation function may be a very narrow one. It appeared desirable to study both these excitation functions in detail with dielectric track detectors using the high-efficiency annular detector geometry reported previously.¹⁵⁻¹⁷ The speed and high sensitivity offered by the spark-scanning procedure for plastic detectors were also well-suited for this purpose.¹⁸

II. EXPERIMENTAL DETAILS

The targets consisted of natural uranium oxide evaporated onto a backing of nickel (1.1 mg/cm²) or aluminum (4.4 mg/cm²). The targets were all thicker than 200 $\mu\text{g}/\text{cm}^2$ of U_3O_8 , i.e., the thickness was greater than the recoil ranges of the products in the target material. Bombardments were made at the tandem Van de Graaff Accelerator at Stony Brook and at the 60-in. cyclotron at the Brookhaven National Laboratory (BNL). Energies up to 28 MeV for the ^4He ions were obtained at Stony Brook, and higher energies at BNL.

The experimental arrangement is shown schematically in Fig. 1. Spontaneously fissioning nuclei that recoil away from the target undergo fission either in flight or after being stopped by the catcher placed downstream. Fission fragments recoiling backward are detected by dielectric track detectors placed on the target cover plate. In the irradiations at Stony Brook, the beam was collimated (3.2-mm diam) and was allowed to hit the target placed in a 3.2-mm aperture. In the BNL experiments the collimator and target apertures were 4.8 and 6.4 mm, respectively. In most experiments the detector plane was displaced 0.79 mm downstream from the target plane.

Makrofol foils weighing ≈ 0.75 mg/cm² were used as detectors in all experiments and were

scanned by the spark-scanning procedure outlined below. Lexan and muscovite mica were used as supplementary detectors in some experiments.

The beam intensity was monitored in one of two ways:

(1) Lexan or mica detectors were used in most of the Van de Graaff experiments to measure the number of prompt fission fragments from the uranium target. Prompt-fission cross-section data from the literature¹⁹ were used to calculate the total number of beam particles striking the target. It was found that the ratio of the integrated beam calculated from the monitor to that obtained from the Faraday cup reading was reasonably constant (variations of about 15%).

(2) In the cyclotron experiments, beam monitoring was accomplished by the measurement of 245-day ⁶⁵Zn produced in natural copper targets exposed to the beam along with the uranium targets. The integrated beam was calculated from the measured intensity of the 1.115-MeV γ ray from the decay of ⁶⁵Zn; the excitation function is known for ⁶⁵Zn in the ⁴He bombardment of copper.²⁰

After exposure the Makrofol detectors were etched in 6.2 *N* NaOH (containing a trace of Dow Benax Surfactant) at 35°C for 6 h. Lexan detectors were etched using the same reagent at 62.5°C for 20 min. Mica strips were annealed at 600°C and then pre-etched in 48% HF at room temperature for 6 h, prior to being used in the experiments. Subsequent to the bombardments, the mica detectors were etched for 20 min in 48% HF at room temperature. Lexan and mica detectors were scanned optically on a Carl Zeiss or Leitz Wetzlar microscope at a magnification of 500.

Rather thin Makrofol foils were used in these experiments and, therefore, most of the fission fragments that hit the detector also penetrated through it. The etching in NaOH developed the

tracks into tiny perforations, and these small holes were scanned in a manner similar to that described by Lark.¹⁸ The optical system of a microscope was removed and in its place a copper needle was mounted to act as the high-voltage electrode. On the moving stage of the microscope, a copper plate was placed to act as the ground electrode. The detector foil was placed on the plate and a high voltage in the range of 1000–1200 V was applied to the needle. Scanning was achieved by moving the foil below the needle after adjusting the distance across the spark gap by means of the focusing system of the microscope. A 500-pF capacitor was connected in parallel with the gap, and the capacitor and gap were charged through a 50-M Ω resistor. As the foil was moved under the needle, sparks were produced whenever a tiny hole came below the needle. The initial sparks enlarged the holes to about 20–30 μ m in diameter and, as Lark noted,¹⁸ prolonged sparking (a few seconds) gave holes visible to the naked eye. Lark used visual scanning of such large holes. A different procedure was followed in this work. Sparking was limited to the first few sparks and an enlarged picture of the detector was taken using a microfilm reader-printer. A magnification of 18.25 was employed. Holes which had diameters of 5–10 μ m became clearly visible in the final picture. Several hundred tracks per square centimeter of detector area could be scanned. The tracks were counted as a function of radial distance from the beam axis.

A detailed discussion of the calculation of the detector efficiency for the annular geometry used in this work is given in Refs. 16 and 17. A short summary of some of the relevant results is given in the Appendix.

III. RESULTS AND DISCUSSION

Bombardments were performed at beam energies from 20 to 40 MeV. Before discussing the observed track distributions and isomer cross sections, we summarize the experimental observations that establish that background effects were not important in these experiments:

- (1) An experiment was performed at 23.7 MeV with only a Ni backing foil. The number of tracks was much less than that observed with a U target.
- (2) When the U target was covered with a thin Ni foil (≈ 1 mg/cm²) a similar reduction in the number of tracks was observed. This Ni was thick enough to stop all recoil products from the target but not the prompt fission fragments.
- (3) The beam intensity varied by a large factor (≈ 40) in a random manner from run to run, but the cross sections obtained were not correlated with this variation.

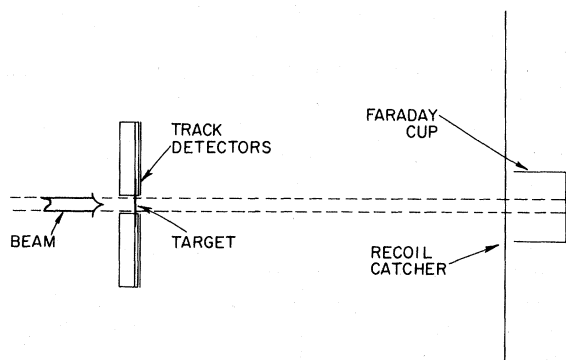


FIG. 1. Schematic diagram of the experimental arrangement. Reaction products that recoil into the region in front of the target could undergo fission and yield tracks in the detectors.

(4) As discussed below, the track distributions and the isomer cross sections varied smoothly with energy.

Items (1) and (2) indicate that the following are not important sources of background: (a) prompt fissions in the uranium target, (b) fission of impurities in the recoil catcher or Faraday cup, (c) fission of uranium impurities in the track detectors induced by stray neutrons. Items (3) and (4) rule out fission of evaporated target material as the source of the observed tracks. The smooth variation with energy of the observed cross sections also provides a strong argument against most sources of background.

A. Radial Distribution of Tracks: Half-Lives

For bombarding energies less than 27 MeV, we have to consider ^{241m}Pu and ^{240m}Pu formed by the ($^4\text{He}, n$) and ($^4\text{He}, 2n$) reactions, respectively. The species ^{241m}Pu has a half-life of 27 μsec ⁶; its contribution to the observed track distribution was found to be very small, particularly for most of the Van de Graaff experiments (recoil catcher at a distance of 247 mm from the target). Thus,

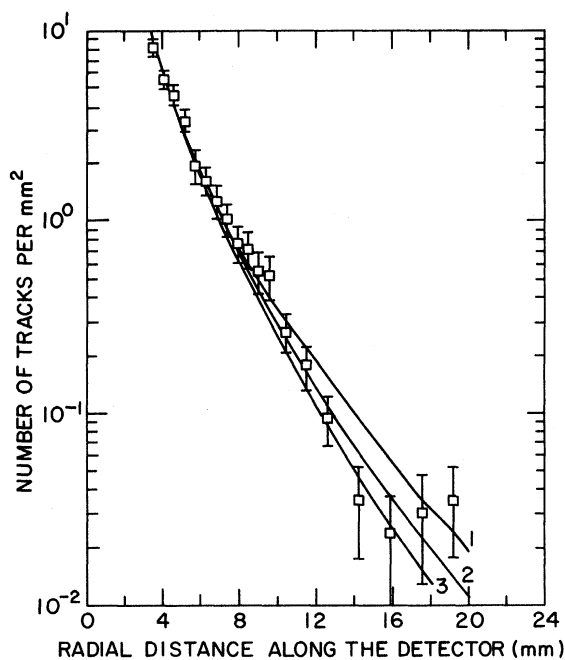


FIG. 2. Experimental track distribution for $^{238}\text{U} + ^4\text{He}$ (bombarding energy 21.9 MeV) compared to various distribution curves, calculated for different values of λ . For all curves, recoil angle = 0° , minimum angle of incidence = 15° . The λ values for curves 1–3 are 0.45, 0.55, and 0.65 mm^{-1} , respectively. The curves are normalized so that they all pass through the experimental points at about 4-mm radius.

at energies less than about 25 MeV, the observed distribution was attributed almost entirely to ^{240m}Pu .

Figure 2 shows the radial distribution of tracks observed for an incident energy of 21.9 MeV, along with three calculated radial distributions obtained according to the procedure summarized in the Appendix. These calculations included the distribution of recoil velocities due to the thick target. On the basis of Fig. 2, we conclude that a value for λ of $0.55 \pm 0.10 \text{ mm}^{-1}$ reproduces the observed radial distribution very well. This gives a half-life of $2.4 \pm 0.5 \text{ nsec}$, a value somewhat smaller than the values of 4.4 ± 0.8 and $3.8 \pm 0.3 \text{ nsec}$ obtained by Vandenbosch and Wolf³ and by Britt *et al.*,⁵ respectively. Both these groups have used electronic timing techniques for the determination of the half-life. This difference is significant but not crucial.

In Fig. 3, the track distribution observed at 22.1 MeV is shown. Here, in addition to the spark-scanning data, the results of extensive optical scanning of a Lexan detector is also shown. With optical scanning the observation cutoff for the angle of incidence is opposite to that for spark scanning. Tracks from particles incident at angles near 90° are not observed because of insufficient

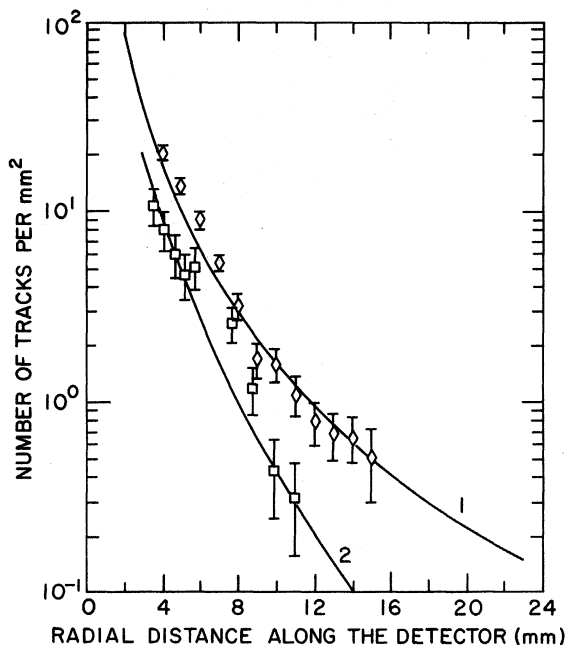


FIG. 3. Comparison of track distributions obtained by spark scanning and optical scanning. Bombarding energy 22.1 MeV. \square : spark scanning of Makrofol. \diamond : optical scanning of Lexan. The curves are calculated for $\lambda = 0.55 \text{ mm}^{-1}$. The minimum angles of incidence are curve (1) 0° and curve (2) 15° .

projected length; also those with incident angle very near 0° might not be observable after chemical etching because of the bulk etching of the surface layer. Both these effects should be small; thus, the distribution calculated for a minimum angle of incidence equal to 0° should fit the observation quite well. In Fig. 3 the calculated distribution is plotted for a λ value of 0.55 mm^{-1} and minimum angle of incidence of 0° . The fit to optical scanning data is quite good, which demonstrates consistency between the two scanning methods.

For incident energies greater than 26 MeV, the track distribution changes in shape as the contribution from 8- μsec $^{239\text{m}}\text{Pu}$ becomes important. The half-life of $^{239\text{m}}\text{Pu}$ is too long to be measured by the recoil technique used here. Essentially all the decays of this isomer come from the recoil catcher, and the track distribution is expected to be essentially flat. Figure 4 indicates that for energies above ≈ 27 MeV, contributions from both $^{239\text{m}}\text{Pu}$ and $^{240\text{m}}\text{Pu}$ have to be considered. These components were resolved by use of a least-square procedure and calculated radial-distribution curves.^{16, 17} The resolved components are displayed in Fig. 4 for incident energies of 28.3 and 33.5 MeV.

B. Excitation Functions

Cross sections for the formation of isomers were calculated at each bombarding energy. The effective target thickness was assumed to be equal to the recoil range of the reaction products in the target material (U_3O_8). The recoil ranges R were obtained using the relation, $R = 1.15 \times R_{\text{LSS}}$, where R_{LSS} is the range calculated according to the procedure of Lindhard, Scharff, and Schiltl.²¹ This

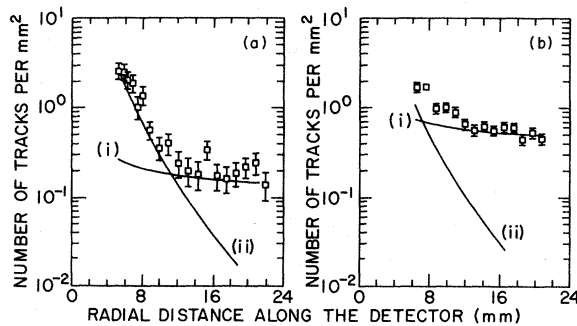


FIG. 4. Resolution of observed track distributions into components of $^{239\text{m}}\text{Pu}$ and $^{240\text{m}}\text{Pu}$. (a) bombarding energy 28.3 MeV. (b) 33.5 MeV. In each case curves (i) and (ii) refer to $^{239\text{m}}\text{Pu}$ and $^{240\text{m}}\text{Pu}$, respectively. The form of these curves was calculated as outlined in the Appendix and in Refs. 16 and 17.

relation was arrived at by comparison of LSS ranges and measured ranges for astatine recoils in bismuth.²² The recoil range was assumed to increase smoothly up to the peak of the excitation function and to remain constant beyond the peak. This assumption was also made on the basis of the behavior of experimental data on the ranges of At recoils in Bismuth.²²

The detector efficiencies needed for the calculation of cross sections were obtained as discussed in the Appendix. In the efficiency calculation, correction was made for the variation of the efficiency with bombarding energy. This correction arises from the change in recoil velocities and therefore λ . The over-all efficiency for $^{240\text{m}}\text{Pu}$ as a function of bombarding energy is given in Table I. These efficiencies are based on the λ value of 0.55 mm^{-1} (21.9-MeV incident energy) deduced from the experimental track distribution. The energy dependence of the efficiency for $^{239\text{m}}\text{Pu}$ is very small because $^{239\text{m}}\text{Pu}$ decays mostly from the recoil catcher. In the choice of the radial function $\epsilon(R, \lambda)$ for each experiment, total momentum transfer was assumed for energies less than the peak of the excitation function and a constant momentum transfer was assumed for higher incident beam energies.

C. $^{238}\text{U}(^4\text{He}, 2n)^{240\text{m}}\text{Pu}$

The cross-section data for this reaction are given in Table II. The uncertainties in the cross sections were computed from the statistical uncertainty in the number of tracks observed and

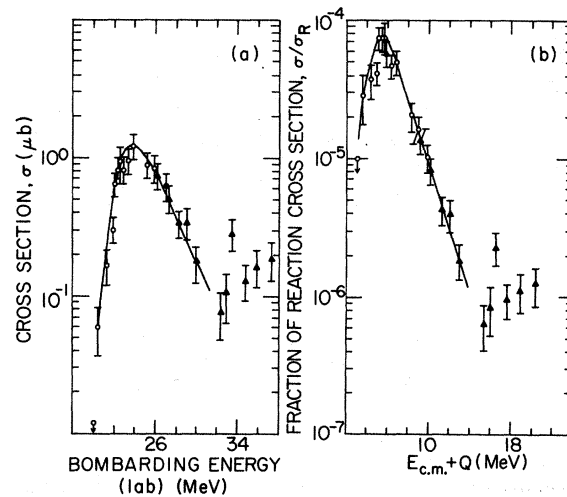


FIG. 5. Excitation function for $^{238}\text{U}(^4\text{He}, 2n)^{240\text{m}}\text{Pu}$: (a) Isomer cross section σ vs bombarding energy in MeV. (b) σ/σ_R vs bombarding energy. The \circ 's refer to Van de Graaff experiments, and \blacktriangle 's to cyclotron experiments.

a 20% over-all uncertainty which includes estimated errors in beam monitoring. The excitation function is displayed in Fig. 5(a). Data points from energies greater than ≈ 30 MeV may well have some contribution from isomers other than ^{240m}Pu (e.g. ^{238m}Pu , see Table V later). In Fig. 5(b) the ratio σ/σ_R is plotted against bombarding energy. Here σ_R is the total reaction cross section for the system $^{238}\text{U} + ^4\text{He}$ calculated from the optical-model code ABACUS.²³ The lines in these figures are smooth lines drawn through the points and do not represent any theoretical predictions. The excitation function in Fig. 5(b) has a full width at half maximum of 4.0 MeV and a full width at $\frac{1}{5}$ maximum of about 6.7 MeV.

In Fig. 6, the excitation function measured in this work is compared with the results of Britt *et al.*⁵ and of Vandenbosch and Wolf.³ Both these groups have used electronic techniques and semiconductor detectors. The peak positions and widths of the excitation functions obtained in the present work agree closely with the results of Britt *et al.*⁵ Our absolute cross sections are about 30% smaller, however. This discrepancy is within the combined uncertainties in the two sets of measurements and thus reasonable agreement is indicated. The cross sections reported by Vandenbosch and Wolf³ do not fall off as rapidly after the peak cross section as do the other two sets.

As noted in the Introduction, an estimate of isomer threshold and excitation energy can be made only with the aid of a model calculation of the excitation function. However, from an examination of Fig. 5(b), a value of $20.0_{-0.5}^{+0.3}$ can be estimated for the threshold (in the lab system) for the production of ^{240m}Pu . Comparison with the ground state Q value²⁴ of 16.62 MeV gives an isomer excitation energy of $3.0_{-0.5}^{+0.3}$ MeV. By comparison to a calculated excitation function, Britt *et al.*⁵ have obtained an excitation energy of 2.6 ± 0.3 MeV for this isomer.

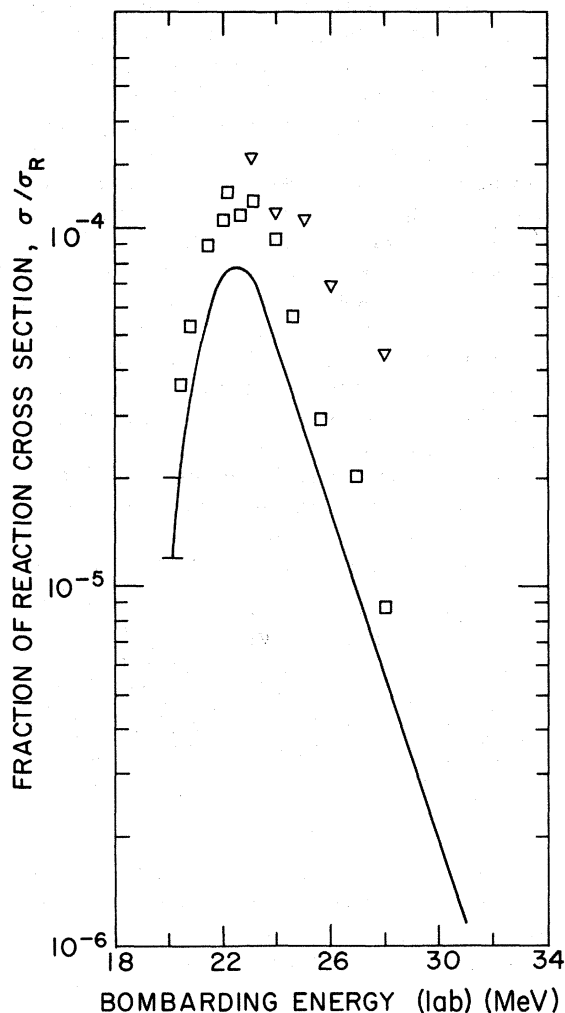


FIG. 6. Comparison of $(^4\text{He}, 2n)$ excitation function measured in this work with the results of other workers. Solid line: same as the line drawn through our points in Fig. 5(b). The points are omitted for the sake of clarity. \square : results of Britt *et al.* (Ref. 5). ∇ : results of Vandenbosch and Wolf (Ref. 3).

TABLE I. Detector efficiency for ^{240m}Pu formed in the reaction $^{238}\text{U}(^4\text{He}, 2n)^{240m}\text{Pu}$.

Bombarding energy (lab) (MeV)	λ (mm^{-1})	Efficiency	
		From radial distance 3.29 to 13.7 mm	From radial distance 4.93 to 13.7 mm
20.0	0.576	0.0468	0.0258
21.0	0.562	0.0500	0.0282
21.9	0.550	0.0543	0.0297
22.5	0.543	0.0560	0.0309
23.0	0.537	0.0571	0.0315
23.5	0.531	0.0580	0.0321

Elwyn and Ferguson²⁵ have reported that neutron bombardment of ^{239}Pu leads to the formation of two ^{240}Pu isomers with half-lives about 5 and 29 nsec. The former may be identified with the 2.4 ± 0.5 -nsec activity described above. Our experiments give no evidence for the formation of the 29-nsec isomer in the reactions of helium ions with ^{238}U . Upper limits to the cross section for formation of this species were determined, and are given in Table III. Elwyn and Ferguson obtained a value of about 0.1 for the ratio of cross sections for the 29 and 5 nsec species produced in the reaction $^{239}\text{Pu}(n, \gamma)^{240m}\text{Pu}$. From Tables II and III we see that in the reaction $^{238}\text{U}(^4\text{He}, 2n)^{240m}\text{Pu}$ this ratio is less than 0.02. Recently, several other groups of workers also have set rather low limits for the cross section for the 29-nsec isomer in charged-particle induced reactions.^{5, 26}

D. $^{238}\text{U}(^4\text{He}, 3n)^{239m}\text{Pu}$

The data for this reaction are summarized in Table IV and plotted in Figs. 7(a) and (b).

In most of the experiments given in Table IV, the target-to-detector distance was 0.8 mm. The observed track distributions were resolved into components due to ^{240m}Pu and ^{239m}Pu . In a few experiments (denoted by asterisks in Table IV) a

TABLE II. Cross-section data for $^{238}\text{U}(^4\text{He}, 2n)^{240m}\text{Pu}$.

Bombarding energy (lab) (MeV)	Isomer cross section σ (μb)	$10^6 \sigma/\sigma_R$
20.0	<0.12	<10
20.5	0.6 ± 0.2	28.7 ± 11.1
21.3	1.7 ± 0.5	37.3 ± 10.6
21.9	3.0 ± 0.6	41.1 ± 8.4
22.1	6.4 ± 1.2	74.8 ± 14.0
22.4	8.2 ± 1.8	75.0 ± 16.1
22.6	9.4 ± 2.4	77.1 ± 19.4
22.8	8.2 ± 1.8	58.1 ± 12.5
23.4	9.5 ± 2.0	47.5 ± 9.8
23.8	12.0 ± 2.5	50.0 ± 10.3
25.3	8.9 ± 1.8	20.9 ± 4.3
26.0	8.4 ± 1.8	16.5 ± 3.6
26.2	7.4 ± 1.5	13.7 ± 2.8
26.8	6.4 ± 1.5	10.3 ± 2.4
27.2	5.1 ± 1.1	8.2 ± 1.8
28.3	3.4 ± 0.8	4.3 ± 1.0
29.1	3.5 ± 0.9	4.0 ± 1.0
30.0	1.8 ± 0.5	1.9 ± 0.5
32.4	0.8 ± 0.3	0.6 ± 0.2
33.0	1.0 ± 0.4	0.8 ± 0.3
33.5	2.9 ± 0.7	2.3 ± 0.6
34.6	1.3 ± 0.4	1.0 ± 0.3
35.9	1.6 ± 0.5	1.1 ± 0.3
37.4	1.9 ± 0.6	1.2 ± 0.4

target-to-detector distance of 9.5 mm was used. In this case the ^{240m}Pu recoils decayed essentially completely before arriving in front of the detector and the observed track distribution could result from only long-lived species like ^{241m}Pu and ^{239m}Pu . In Fig. 7(b) the threshold for the formation of ^{239m}Pu is somewhat obscured by the appreciable cross section in the 24–27-MeV region that may be partly attributed to ^{241m}Pu . Statistical uncertainties are also quite large in the experiments at energies lower than 27 MeV. Over the energy region from 27 to 37 MeV [covered by the line in Fig. 7(b)] the excitation function is determined with reasonably good precision. The full width at half maximum of this excitation function is about 7 MeV. A more precise measurement in the energy region from 25 to 27 MeV is required to allow an accurate evaluation of the threshold for ^{239m}Pu . As noted above, interference from ^{241m}Pu is the most serious difficulty in this region. The present results allow us to estimate that the threshold is 26.0 ± 1.0 MeV, which leads to the estimate of 2.5 ± 1.0 MeV for the excitation energy of ^{239m}Pu . (Q value for ground state is 23.07 MeV.²⁴)

In Fig. 8 the ^{239m}Pu excitation function determined in this work is compared with the results of Britt *et al.*⁵ and of Vandenbosch and Wolf.³ Wolf and Unik have recently reported a cross section of $33.4 \mu\text{b}$ for the reaction $^{238}\text{U}(^4\text{He}, 3n)^{239m}\text{Pu}$ at 31.4 MeV.²⁷ At energies lower than 27 MeV, we obtain somewhat larger cross sections for the sum of ^{241m}Pu plus ^{239m}Pu than those determined by Britt *et al.*⁵ Both measurements, nevertheless, indicate the onset of ^{239m}Pu formation at the same energy (≈ 27 MeV). Britt *et al.* determined only the rising edge of the ^{239m}Pu excitation function. The highest cross sections they have determined are in agree-

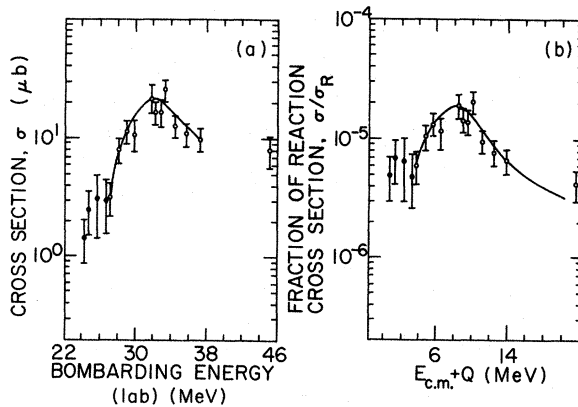


FIG. 7. Excitation function for $^{238}\text{U}(^4\text{He}, 3n)^{239m}\text{Pu}$: (a) cross section in microbarns vs bombarding energy in MeV. (b) σ/σ_R vs bombarding energy. ●: Van de Graaff experiments. ○: cyclotron experiments.

ment with the corresponding measurements made in the present work. Vandenbosch and Wolf reported relative cross sections at six energies and an approximate isomer ratio. Using this isomer ratio, their results were converted into the appropriate units and plotted in Fig. 8. These results seemed to indicate an excitation function that is quite narrow with a full width at half maximum of 3 to 3.5 MeV. The more complete measurements made here show that the excitation function is certainly not this narrow although it is probably more narrow than that for the ground state. The suggestion of very narrow excitation functions for fission isomers was also made by Natowitz and Archer²⁸ from a study of isomers produced in helium ion bombardments of ²³⁷Np. The present study does not support these earlier indications for a very small width of the excitation functions.

E. ²³⁸U(⁴He, 4n)^{238m}Pu

Vandenbosch and Wolf³ have searched for ^{238m}Pu in the ⁴He bombardment of ²³⁸U with negative results. They concluded that if the isomer ratio is 5×10^{-4} , the half-life of ^{238m}Pu must be less than 2 nsec. Britt *et al.*⁵ have reported the formation of an isomer of ^{238m}Pu with a half-life of 6.5 nsec from the reaction ²³⁶U(⁴He, 2n)^{238m}Pu. Recently, Limkilde and Sletten²⁹ have observed a 0.5-nsec fission isomer in the reaction ²³⁶U(⁴He, 2n)^{238m}Pu. This new ²³⁸Pu isomer was assigned as the ground state in the second well. The 6.5-nsec ²³⁸Pu discovered by Britt *et al.*⁵ was also observed by Sletten and colleagues, and it was established that the threshold for the production of 6.5-nsec isomer was higher than that for the 0.5-nsec isomer was thus taken to be an excited state in the second well.

In Tables V and VI upper limits to the cross section for 6.5-nsec ^{238m}Pu are given. These limits were obtained by assuming that the short-lived component was entirely 6.5-nsec ^{238m}Pu. The efficiency of the present arrangement was rather low for the 0.5-nsec isomer and only rather large upper limits could be established for the cross

TABLE III. Cross-section limits for 29-nsec ^{240m}Pu.

Bombarding energy (lab) (MeV)	Upper limit for isomer cross section, $\sigma(\mu\text{b})$
21.9	<0.05
23.4	<0.28
25.3	<0.18
26.0	<0.14

TABLE IV. Cross-section data for ²³⁸U(⁴He, 3n)^{239m}Pu.

Bombarding energy (lab) (MeV)	Isomer cross section $\sigma(\mu\text{b})$	$10^6 \sigma/\sigma_R$
24.3 ^a	<1.5 ± 0.6	<5.0 ± 2.0
24.8 ^a	<2.6 ± 1.0	<7.0 ± 2.8
25.8 ^a	<3.2 ± 1.8	<6.6 ± 3.6
26.8 ^a	<3.1 ± 1.5	<5.0 ± 2.4
27.2	3.3 ± 1.0	6.0 ± 1.8
28.3	8.1 ± 1.9	10.3 ± 2.4
29.1	11.6 ± 2.6	13.3 ± 3.0
30.0	10.9 ± 3.2	11.5 ± 3.4
32.0	21.8 ± 5.0	19.3 ± 4.4
32.4	16.6 ± 3.5	14.2 ± 3.0
33.0	16.9 ± 4.2	13.9 ± 3.5
33.5	26.0 ± 5.4	20.6 ± 4.3
34.6	13.0 ± 2.7	9.6 ± 2.0
35.9	11.1 ± 2.5	7.8 ± 1.8
37.4	10.0 ± 2.2	6.6 ± 1.5
45.3	8.0 ± 2.4	4.2 ± 1.2

^aThe target-to-detector distance was 9.5 mm compared to 0.8 mm for the other experiments.

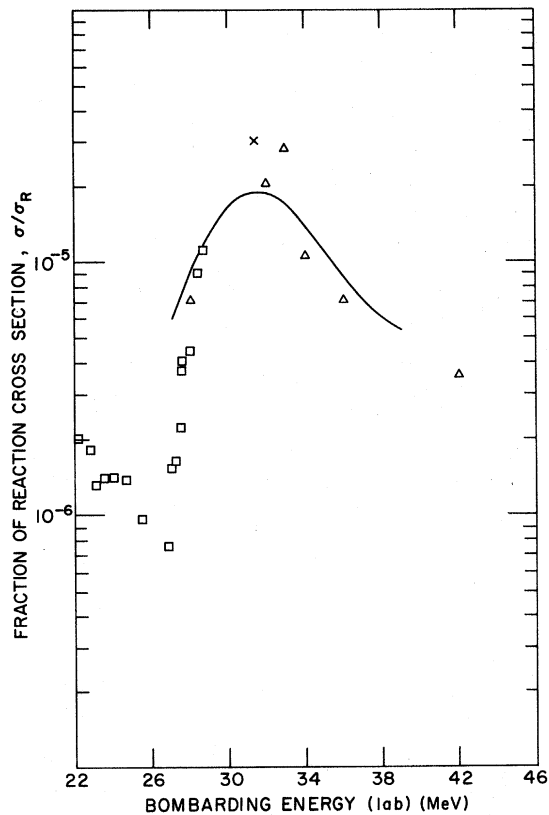


FIG. 8. Comparison of the (⁴He, 3n) excitation functions measured in this work with the results of other workers. Solid line: the same as the smooth line in Fig. 7(b). □: Britt *et al.* (Ref. 5). △: Vandenbosch and Wolf (Ref. 3). ×: Wolf and Unik (Ref. 27).

section of this isomer. Tables V and VI give cross-section limits obtained by assuming that the short-lived component in the track distribution arises from either of the ^{238}Pu isomers.

A more general discussion of the results of this study is included in the accompanying paper.¹³ Comparison of the excitation functions to statistical model calculations is in progress.¹⁴

ACKNOWLEDGMENTS

Thanks are due C. P. Baker and the operating crew of the BNL cyclotron and to L. Lee and E. Schultz of the Stony Brook tandem Van de Graaff. The scanning work of A. Campo, G. R. Namboodiri, and J. Wolf is greatly appreciated. Helpful discussions with Dr. J. B. Cumming and the use of some of his targets are also appreciated.

APPENDIX

Here we present a brief outline of the efficiency calculations for the detector arrangement used in this work (see Fig. 1). Additional details may be found in Refs. 16 and 17.

The etching and sparking conditions employed are such that all fission fragments incident on the detector at angles greater than a certain minimum value are detected. Experimental measurements show that for fission fragments from the reaction $^{238}\text{U} + ^4\text{He}$, this minimum angle is 15° .¹⁶

Initially, let us assume that the recoils travel in the beam direction without angular divergence; also let us neglect the finite beam size. Thus, the path of the recoils coincides with the beam axis. Moreover, the target and detector are assumed to be in the same plane. We define the quantity λ by the relation

$$\lambda = \frac{\ln 2}{D_{1/2}} = \frac{\ln 2}{VT_{1/2}}, \quad (\text{A1})$$

where V , $T_{1/2}$, and $D_{1/2}$ are the recoil velocity, half-life, and half-decay distance of the recoils.

The number of fission fragments N_R that arrive

at unit area of the detector at radius R is given by

$$N_R = N\epsilon(R, \lambda), \quad (\text{A2})$$

where N is the total number of isomer recoils and

$$\epsilon(R, \lambda) = \left(\frac{\lambda}{2\pi}\right) \int_{D_{\min}}^{D_c} D e^{-\lambda D} (D^2 + R^2)^{-3/2} dD + \left(\frac{1}{2\pi}\right) D_c e^{-\lambda D_c} (D_c^2 + R^2)^{-3/2}. \quad (\text{A3})$$

The variable D denotes distance along the flight path, measured from the target-detector plane. The first term on the right-hand side of Eq. (A3) gives the contribution from isomer nuclei fissioning in flight, while the second term represents the contribution from recoils that come to rest on a catcher before undergoing fission. The distance between the catcher and the target-detector plane is D_c . It may be noted that $\epsilon(R, \lambda)$ is the number of fission fragments detected per unit area at a radial distance R when the number of isomer recoils emerging from the target is unity. In Eq. (A3) it is assumed for simplicity that the fission fragments are emitted isotropically. The value of D_{\min} is determined by the minimum angle criterion mentioned above.

Equation (A3) defines the radial track distribution as a function of λ . A number of distributions have been obtained by numerical integration of Eq. (A3). The track distribution can be used to deduce isomer half-life, particularly for λ values in the range 1 to 0.01 mm^{-1} [corresponding to the half-life range of ≈ 1 to ≈ 100 nsec in the case of ($^4\text{He}, xn$) reactions on heavy elements].

The over-all detector efficiency E_λ can be obtained by integration of the radial distribution between appropriate values of R :

$$E_\lambda = 2\pi \int_{R_1}^{R_2} \epsilon(R, \lambda) R dR. \quad (\text{A4})$$

This experimental arrangement offers quite high detector efficiencies ($>2\%$) over a wide range

TABLE VI. Cross-section limits for ^{238m}Pu . Short-lived component resolved into 0.9- and 6.5-nsec components.

Bombarding energy (lab) (MeV)	Cross-section limits (μb)	
	0.9-nsec isomer ^a	6.5-nsec isomer
33.0	<34	<0.18
33.5	<33	<0.45
34.6	<30	<0.35
35.9	<10	<0.38
37.4	<36	<0.43

^a The limits for the shorter-lived species would be somewhat greater if the half-life was taken as 0.5 nsec.

TABLE V. Cross-section limits for ^{238m}Pu . Entire short-lived component assigned as 6.5-nsec ^{238m}Pu .

Bombarding energy (lab) (MeV)	Cross-section limit for 6.5-nsec ^{238m}Pu (μb)
33.0	<0.24
33.5	<0.65
34.6	<0.47
35.9	<0.42
37.4	<0.64

of isomer half-decay distances ($1 \text{ mm} < D_{1/2} < 30 \text{ cm}$).

For simplicity we excluded from the above discussion the following effects: (1) the distribution of recoil velocities, (2) anisotropic angular distribution of fission fragments, and (3) angular divergence of isomer recoils from the beam axis. Item (1) is particularly important in thick-target experiments of the kind reported here. The recoils emerge from the target with velocities ranging from near zero to the maximum possible value. This effect has been taken into account by numerical integration over a target imagined to consist of many layers and considering recoils originating from the different layers separately. The detector efficiencies used in the present work were actually obtained in this manner. Corrections

were also calculated for effects (2) and (3) mentioned above; these corrections were, in fact, very small.

In order to measure the cross sections of two separate fission isomers produced in the same irradiation, the radial track distributions may be resolved into components. (See Fig. 4.) The procedure follows very closely the methods used for radioactive decay for each component as a function of time. The calculated efficiency as a function of R is fitted to the sum of two exponentials. Thus, if two species of known half-life are produced, the radial track distribution is fitted by least squares to the sum of the two calculated efficiency curves. More details and results of these calculations are given in Ref. 17. The authors will supply on request the listings of the programs used.

*Work supported by U. S. Atomic Energy Commission.

†Present address: Cyclotron Institute, Texas A&M University, College Station, Texas.

‡Present address: Nuclear Radiation Center and Department of Chemistry, Washington State University, Pullman, Washington 99163.

¹S. M. Polikanov, V. A. Druin, V. A. Karnaukov, V. L. Mikheev, A. Pleve, N. K. Skobolev, V. G. Subbotin, G. M. Ter-Akop'yan, and V. A. Fomichev, *Zh. Eksperim. i Teor. Fiz.* **42**, 1464 (1962) [transl.: *Soviet Phys. - JETP* **15**, 1016 (1962)].

²See J. R. Huizenga, *Science* **168**, 1405 (1970).

³R. Vandenbosch and K. L. Wolf, in *Proceedings of the Second International Atomic Energy Symposium on Physics and Chemistry of Fission, Vienna, Austria, 1969* (International Atomic Energy Agency, Vienna, Austria, 1969); K. Wolf, Ph.D. thesis, Univ. of Washington, Seattle, 1968 (unpublished).

⁴N. L. Lark, G. Sletten, J. Pedersen, and S. Bjørnholm, *Nucl. Phys.* **A139**, 481 (1969).

⁵H. C. Britt, S. C. Burnett, B. H. Erkkila, J. E. Lynn, and W. E. Stein, *Phys. Rev. C* **4**, 1444 (1971); S. C. Burnett, H. C. Britt, B. H. Erkkila, and W. E. Stein, *Phys. Letters* **31B**, 523 (1970).

⁶S. M. Polikanov and G. Sletten, *Nucl. Phys.* **A151**, 656 (1970).

⁷S. Bjørnholm and V. M. Strutinsky, *Nucl. Phys.* **A136**, 1 (1969).

⁸S. G. Nilsson, C. F. Tsang, A. Sobczewski, Z. Szymanski, S. Wycech, C. Gustafson, I. L. Lamm, P. Moller, and B. Nilsson, *Nucl. Phys.* **A131**, 1 (1969).

⁹M. Brack, J. Damgaard, A. S. Jensen, H. C. Pauli, V. M. Strutinsky, and C. Y. Wong, *Rev. Mod. Phys.* **44**, 320 (1972).

¹⁰S. Bjørnholm, J. Borggreen, L. Westgaard, and V. A. Karnaukhov, *Nucl. Phys.* **A195**, 513 (1967).

¹¹S. Jagåre, *Phys. Letters* **32B**, 571 (1970); *Nucl. Phys.* **A137**, 241 (1969).

¹²R. Vandenbosch, *Phys. Rev. C* **5**, 1428 (1972).

¹³A. Fleury, F. H. Ruddy, M. N. Namboodiri, and J. M. Alexander, following paper, *Phys. Rev. C* **7**, 1231 (1973).

¹⁴E. R. Jones, III, A. Fleury, and J. M. Alexander, private communication.

¹⁵F. H. Ruddy, M. N. Namboodiri, and J. M. Alexander, *Phys. Rev. C* **3**, 972 (1971).

¹⁶M. N. Namboodiri, Ph.D. thesis, State University of New York at Stony Brook, 1972 (unpublished).

¹⁷M. N. Namboodiri, F. H. Ruddy, and J. M. Alexander, to be published in *Nucl. Instr. Methods*, 1973.

¹⁸N. Lark, *Nucl. Instr. Methods* **67**, 137 (1969).

¹⁹J. R. Huizenga, R. Vandenbosch, and H. Warhanek, *Phys. Rev.* **124**, 1964 (1961); V. Viola and T. Sikkeland, *Phys. Rev.* **128**, 767 (1962).

²⁰F. H. Ruddy, Ph.D. thesis, Simon Fraser University, Burnaby, British Columbia, 1968 (unpublished).

²¹J. Lindhard, M. Scharff, and H. E. Schiott, *Kgl. Danske Videnskab. Selskab, Mat. - Fys. Medd.* **33**, No. 14 (1963).

²²P. D. Croft and J. M. Alexander, unpublished results.

²³E. H. Auerbach, Brookhaven National Laboratory, unpublished. Real well depth 50 MeV; imaginary well depth 27 MeV, volume absorption; interaction radius $1.17 A^{1/3} + 1.77$.

²⁴J. H. E. Mattauch, W. Thiele, and A. H. Wapstra, *Nucl. Phys.* **67**, 1 (1965).

²⁵A. J. Elwyn and A. T. G. Ferguson, *Nucl. Phys.* **A148**, 337 (1970).

²⁶Private communications from R. Vandenbosch and G. Sletten quoted by V. Metag, R. Repnow, and P. von Brentano, *Nucl. Phys.* **A165**, 289 (1971).

²⁷K. L. Wolf and J. P. Unk, *Phys. Letters* **38B**, 405 (1972).

²⁸J. B. Natowitz and J. K. Archer, *Phys. Letters* **30B**, 463 (1969).

²⁹P. Limkilde and G. Sletten, in *Proceedings of the European Conference on Nuclear Physics, Aix-en-Provence, France, June 1972* (unpublished).